Nanotechnology, Science and Applications

Dovepress
open access to scientific and medical research

Open Access Full Text Article

ORIGINAL RESEARCH

Surface-functionalized cockle shell–based calcium carbonate aragonite polymorph as a drug nanocarrier

This article was published in the following Dove Press journal:
Nanotechnology, Science and Applications
16 May 2017
Number of times this article has been viewed

Syairah Liyana Mohd Abd Ghafar[1]
Mohd Zobir Hussein[2]
Yaya Rukayadi[1,3]
Md Zuki Abu Bakar Zakaria[1,4]

[1]Institute of Bioscience, [2]Institute of Advance Technology, [3]Department of Food Science, Faculty of Food Science and Technology, [4]Department of Veterinary Preclinical Sciences, Faculty of Veterinary Medicine, Universiti Putra Malaysia, Serdang, Selangor, Malaysia

Abstract: Calcium carbonate aragonite polymorph nanoparticles derived from cockle shells were prepared using surface functionalization method followed by purification steps. Size, morphology, and surface properties of the nanoparticles were characterized using transmission electron microscopy, field emission scanning electron microscopy, dynamic light scattering, zetasizer, X-ray powder diffraction, and Fourier transform infrared spectrometry techniques. The potential of surface-functionalized calcium carbonate aragonite polymorph nanoparticle as a drug-delivery agent were assessed through in vitro drug-loading test and drug-release test. Transmission electron microscopy, field emission scanning electron microscopy, and particle size distribution analyses revealed that size, morphology, and surface characterization had been improved after surface functionalization process. Zeta potential of the nanoparticles was found to be increased, thereby demonstrating better dispersion among the nanoparticles. Purification techniques showed a further improvement in the overall distribution of nanoparticles toward more refined size ranges <100 nm, which specifically favored drug-delivery applications. The purity of the aragonite phase and their chemical analyses were verified by X-ray powder diffraction and Fourier transform infrared spectrometry studies. In vitro biological response of hFOB 1.19 osteoblast cells showed that surface functionalization could improve the cytotoxicity of cockle shell–based calcium carbonate aragonite nanocarrier. The sample was also sensitive to pH changes and demonstrated good abilities to load and sustain in vitro drug. This study thus indicates that calcium carbonate aragonite polymorph nanoparticles derived from cockle shells, a natural biomaterial, with modified surface characteristics are promising and can be applied as efficient carriers for drug delivery.

Keywords: cockle shell, calcium carbonate, aragonite, surface functionalization, nanoparticle, drug delivery

Introduction

Drug-delivery system is no longer a new branch of study in science today. It is already commonplace and yet it is still being extensively studied. Drug-delivery studies are interdisciplinary and cover vast array of disciplines including biology, chemistry, physics, pharmaceutical chemistry, and biomedical sciences combined with engineering and biotechnology fields as well.[1–8] One of the most important aspects of drug-delivery system is the role of drug vehicles.[9–11] In fact, numerous drug carriers have been invented since the past decades using various materials such as inorganic nanomaterials, carbon nanotubes, gold, silver, and polymer-based nanoparticles.[7–24] Although there are various choices of materials, calcium carbonate is used as one of the most common inorganic materials to devise few delivery vehicles in drug-delivery system.[8,12–14,21–24] On top of that use of bio-based calcium carbonate materials in the

Correspondence: Md Zuki Abu Bakar Zakaria
Institute of Bioscience, Universiti Putra Malaysia, Serdang, 43400, Selangor, Malaysia
Tel +60 389 472 102
Fax +60 389 472 101
Email syerra_saffar@hotmail.com

development of drug carriers is gradually gaining enormous attention among researchers year by year.[8,21,22]

In general, a large number of studies have been conducted to investigate the special properties of calcium carbonate material.[12,23,25–33] Moreover, it has been widely documented that calcium carbonate exists in three kinds of polymorphs: calcite, aragonite, and vaterite.[27,29,31,33,34] Each polymorph indeed possesses unique properties that can be exploited for various industrial purposes. Nevertheless, calcium carbonate aragonite polymorph recently has become a center of attention among scientists, especially among those in biomedical and pharmaceutical fields, and has been explored for its numerous physical and chemical aspects to be used in many versatile applications.[34–36]

Many studies have demonstrated that aragonite polymorph of calcium carbonate has high potential to be used as an excellent biomedical material.[34,36–39] In fact, aragonite is denser than calcite, is sensitive toward temperature change, has various morphologies, has high mechanical strength, and also is both biodegradable and biocompatible, though it is thermodynamically less stable than calcite at ambient temperature and pressure.[34,37–41] Therefore, these special properties of calcium carbonate aragonite polymorph have recently been manipulated for diverse potential applications in many fields, especially in biomedical research including drug delivery[8,21,22] and bone tissue engineering.[35,36]

To date, it has become a trend to use natural materials primarily in constructing and designing carriers for drug-delivery system.[8,21,22] The utilization of bio-based materials such as mineral products[42,43] and the shells from naturally occurring organisms[8,21,22,34–36,39–41,44–46] as raw materials in the development of various biomedical tools has generated great interest due to environmentally friendly characteristics, these days. For example, over the past two decades,[40,44,45] coral (*Porites sp.*) was documented as a main biomaterial source for bone substitute. However, several years later, a comparative study[40] found that cockle shells had mineral composition similar to corals and, therefore, cockle shell was suggested as a compatible alternative biomaterial source for bone graft.

Moreover, another study[41] discovered that cockle shells that were collected from the West Coast of Peninsular Malaysia consisted of 98.7% of calcium carbon (CaC) elements of the total mineral compositions and the remaining 1.3% composition was made of magnesium (Mg), sodium (Na), phosphorus (P), potassium (K), and other mineral components including iron (Fe), copper (Cu), nickel (Ni), boron (B), zinc (Zn), and silicon (Si). Likewise, a recent study by Bharatham et al[36] was also in accordance with these findings and agreed that cockle shell is composed of significantly high content of CaC minerals. In fact, they also revealed that their analysis on heavy metal elements including mercury (Hg), arsenic (As), cadmium (Cd), and lead (Pb) were found to be below detection limits in cockle shells according to Standard Specification for Composition of Hydroxyapatite for surgical implants based on American Society Requirements for Testing and Materials.[36] This finding, therefore, justifies that cockle shell is safe for human consumption and has a remarkable potential particularly in orthopedic and other biomedical applications.[35,36,40,41]

Furthermore, the abundant amount of shells due to the high yearly production and consumption of cockles in the food industry, offers a convenient and low cost biomaterial source (cockle shells), that are widely available in many Asian countries.[41] Moreover, recycling the dumped cockle shells is one of the most effective ways to reuse and exploit their mineral resources, besides effectively preserving the environment as well. To date, cockle shell is being exploited as a material for biocomposite scaffold in bone tissue engineering, which evidences its ability as a good-quality biomaterial of calcium carbonate aragonite polymorph.[35] In fact, the abilities of calcium carbonate aragonite polymorph nanoparticles derived from cockle shells as a delivery agent have been successfully demonstrated for anticancer drug-carrier therapy[8,22] and also integrated with an antibiotic drug[21] in recent years.

However, the journey to investigate the physical and chemical properties of the delivery agents remains ongoing over the years as many aspects of delivery vehicles should be profoundly studied to gain better understandings on the efficient characteristics of the delivery vehicle so that an applicable and effective delivery agent can be designed.[8,21,22] The exploration for remarkable delivery vehicles has definitely been an interesting yet challenging area of research over the past few decades with many progressive developments of drug vehicles that are initially made of various types of biomaterials from micron-sized particles and currently advancing to more engineered constructs of nanoparticle delivery carriers nowadays. Besides the type of materials, size and surface properties are some of the important factors of a drug-delivery system. These factors play significant roles in determining the distribution of therapeutic molecules, ability of drug targeting, stability of carrier particles, and their pivotal capacities to load and release drug compounds.[2,3,5,7,9–11] Many reports in the literature have proven that nanoparticles present more advantages in drug-delivery system compared

to micron-sized particles in terms of several aspects including distribution, protection, targeting, and clearance abilities in systemic circulation.[4,5,10,24]

Moreover, another important characteristic of a delivery carrier is that the surface feature of carrier particles essentially determines driving forces such as electrostatic, hydrophilic, and hydrophobic forces for drug interaction to the carrier and can also influence cellular interactions within the body.[9] Furthermore, many previous works have proved that various functional applications of calcium carbonate compound generally depend on its controlled surface properties.[30,42,47–50] Additionally, surface functionalization has been documented to improve the interaction between carriers and specific cell membranes by manipulating the surface charges of particles, thereby helping the delivery carrier approaching the targeted site of action efficiently during systemic vascular circulation.[2,3,7,9–11] The interaction between the carrier's particles and drug compounds in suspension can be enhanced through some exploitation on their surface properties.[7,9–11,24] Such modification will thus affect the surface energy and electrical potential of particles, thereby improving their dispersion as well as distribution in general.[47,49–52]

Therefore, the ability and efficacy of cockle shells–based calcium carbonate aragonite polymorph nanoparticles with surface functionalization as a delivery carrier will be herein investigated to explore its possible potentials in drug-delivery application. This research employs some basic procedures to produce the nanoparticles based on the established production method[39,46] with some improvements in the synthesis method. Furthermore, a specific and improved modification process[47] was also incorporated into the production method in order to uniformly produce and effectively functionalize the surface of cockle shell–based calcium carbonate aragonite polymorph nanoparticles. This will attain the permissible necessities as a potential nanocarrier which is equipped with efficient delivery bioactivities.

The main scope of this study was to synthesize nanoparticles with homogenous size and better surface characterization derived from cockle shells, particularly for safe and feasible drug-delivery applications. In this regard, a few physical and chemical aspects of the nanoparticle products prepared in the presence of dodecyl dimethyl betaine (BS-12) were thus evaluated for practical application of drug delivery. Characteristics of delivery carriers that would be appropriately assessed in this study include physical size and morphological components of the nanoparticles, surface properties, cytotoxicity, and their loading and release abilities as efficient delivery vehicles. These assessments are in fact very crucial while designing cockle shell–based calcium carbonate aragonite polymorph nanocarrier so that it can be classified as a promising delivery agent that achieves stringent requirements as stable, safe, and efficient drug carriers in drug-delivery colloidal system.

Materials and methods

Synthesis of surface-functionalized cockle shell–based calcium carbonate aragonite polymorph nanoparticles

Micrometer-sized particles from cockle shells was prepared according to previous studies.[39,46] The particles thus obtained were further processed into nanoparticles according to a previously described method.[46] BS-12 was purchased from Shanghai Jindun Industrial Company, Shanghai, People's Republic of China. Deionized water was obtained from Elga Pure lab intelligent pure water purification system (Model Ultra GE MK2, UK) with 18.2 MΩ-cm resistivity of water purity.

A total of 5 g of cockle shell–based calcium carbonate microparticles were mixed with 50 mL of distilled water in a 250 mL conical flask. The suspension was then stirred vigorously at 1200 rpm for 1 hour at room temperature using a mechanical magnetic stirrer hotplate (WiseStir SMHS; Witeg Labortechnik GmbH, Germany, and magnetic stirrer bar) and 1.5 mL of BS-12 was added to the suspension and stirred again at 1000 rpm for 2 hours at room temperature. After that the resulting suspension was centrifuged several times to wash out BS-12 residues from the suspension (Multifuge 3S-R, model D-37520; Thermo Fisher Scientific, Waltham, MA, USA) and the sample was dried in an oven for 2 days at 80°C.

Next, surface functionalization was carried out according to a previously described method.[47] Calcium chloride dihydrate ($CaCl_2{\cdot}2H_2O$) was bought from Friedemann Schmidt Chemical. A total of 20 g of cockle shell–based calcium carbonate aragonite polymorph spherical nanoparticle was suspended into 80 mL calcium chloride dihydrate solution ($CaCl_2{\cdot}2H_2O$) prepared at 1000 parts per million concentration in a 250 mL glass bottle with a cap. The suspension was then sonicated three times for 15 minutes, each time using an ultrasonic probe (Model 2510; Sigma-Aldrich Co., St Louis, MO, USA) with a resting period of 20 minutes between sonication treatment intervals. The bottle was then tightly sealed and agitated for 6 hours at 200 rpm on a roller mill machine (Labcampus company, Korea) for 5 days at room temperature. The sample was then washed, centrifuged, and then dried in an oven at 80°C for 2 days.

The surface-functionalized cockle shell–based calcium carbonate aragonite polymorph spherical nanocarriers were filtered two times during purification process. Approximately 5 g of surface-functionalized cockle shell–based calcium carbonate aragonite nanoparticle powder was added to 200 mL of deionized water and sonicated for 15 minutes to obtain a uniform particle distribution in suspension. After that the sample was first prefiltered by a membrane filter with a pore size of 5 μm (cellulose nitrate membrane filter; Sartorius, Göttingen, Germany) using a vacuum filtration set (47 mm filtration assembly with 300 mL funnel, 1 L flask) connected to an oil-free vacuum pump (Rocker Scientific Co., Ltd. New Taipei City, Taiwan). Subsequently, the filtrate was collected and refiltered for the second time again by a membrane filter with a pore size of 0.1 μm (cellulose acetate membrane filter; Sartorius) using the same vacuum filtration set. Then, the sample was cooled at −20°C for 24 hours in several 30 mL sterile containers and placed in a freeze-drying machine (Model Christ Alpha 1–2 LD plus; Martin Christ Gefriertrocknungsanlagen GmbH, Osterode am Harz, Germany) for 5 days. Finally, the dried surface-functionalized cockle shell–based calcium carbonate aragonite nanoparticle sample was collected for further studies. In short, the whole experimental procedure is summarized in Figure 1.

Drug-loaded surface-functionalized cockle shell–based calcium carbonate aragonite polymorph nanocarrier

A total of 5 mg of surface-functionalized cockle shell–based calcium carbonate aragonite nanoparticles was accurately

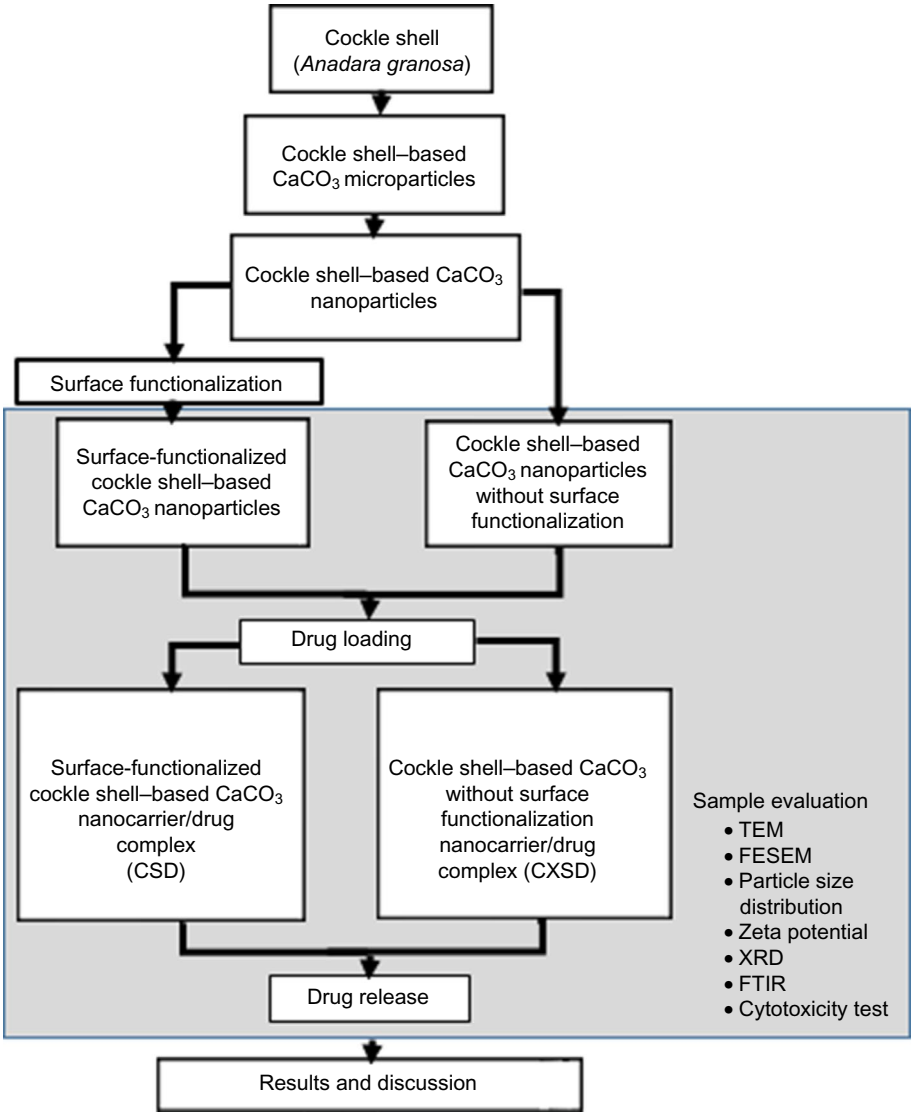

Figure 1 Flowchart of the experimental procedures.
Abbreviations: TEM, transmission electron microscopy; FESEM, field emission scanning electron microscopy; XRD, X-ray diffraction; FTIR, Fourier transform infrared spectrometry; CSD, cockle shell-based $CaCO_3$ nanocarrier with surface functionalization loaded drug; CXSD, cockle shell-based $CaCO_3$ nanocarrier without surface functionalization loaded drug.

weighed and added to 1 mL of phosphate-buffered saline (PBS) at pH 7.4 in a microcentrifuge tube to make a final concentration of 5 mg/mL. Nanocarrier and drugs in ratios 5:1, 5:2, 5:3, and 5:5 were weighed and dissolved, respectively, into each microcentrifuge tube, and the mixtures were continuously shaken at 200±1 rpm using an orbital shaker (Protech Model 719; Tech-Lab Scientific, Cheras, Malaysia) overnight at room temperature. Then, the nanoparticle/drug complexes were washed, centrifuged, and oven-dried (FD 115; Fisher Scientific, Limburg, Germany) at 50°C. The supernatant of each formulated mixture was collected for further analysis. These procedures were repeated for cockle shell–based calcium carbonate aragonite nanoparticles without surface modification for comparison purposes. All the experiments were conducted in three different experimental batches.

Physicochemical characterization

The size and shape of samples were evaluated using a transmission electron microscopy (TEM) (H-7100 Transmission Electron Microscope, Hitachi, Tokyo, Japan) operated at a voltage of 150 kV. The sample was first mixed with absolute alcohol and sonicated using a sonicator (Power Sonic 505, Hwashin Technology Co., Gangnam-gu, South Korea) for 30 minutes. Then, a drop of the colloidal solution was put onto a carbon-covered copper grid placed on a piece of filter paper and dried at room temperature for an hour.

Surface morphology and nanostructure of the sample were examined using a field emission scanning electron microscopy (JOEL 7600F Scanning Electron Microscope, JOEL USA, Inc., USA) operated at a voltage of 5 kV. All the samples were dispersed onto carbon conductive adhesive placed on sample holders and then coated with platinum before examining under electron microscope.

Zeta potential and size distribution analyses of nanoparticles were performed using a Zetasizer Nano ZS device (Malvern Instruments Ltd., Malvern, UK). Each sample was prepared using deionized water and dispersed using an ultrasonicator prior to measurements. Particle size distribution and zeta potential measurements were carried out using disposable cuvettes at room temperature with dynamic light scattering detected at an angle of 173°. Both size distribution and zeta potential of each sample were averaged and expressed as mean±standard deviation of three replicate measurements.

Crystalline properties of the samples were investigated by X-ray powder diffractometer (Model PW 3040/60, MPD X'pert High Pro PANalytical; Philips) equipped with a Cu-K (λ=0.15406 nm) radiation source scanned at a rate of 40/minute. The phase of each sample was determined at 2θ=5°–60° at room temperature.

Chemical analyses of the samples were performed using a Fourier transform infrared spectrometer (FTIR; Model Spectrum 100; Perkin Elmer, Waltham, MA, USA) over a range of 280–4000 cm^{-1} at 2 cm^{-1} resolution.

Determination of drug-loading capacity and encapsulation efficiency

Drug loading capacity and encapsulation efficiency of each sample were determined by calculating the differences between the total weight of drug fed (Wt) and the amount of free drug (Wf) in the supernatant using Equations (1) and (2):

$$\text{Loading content} = \frac{\text{Wt} - \text{Wf}}{\text{Wnp}} \times 100 \quad (1)$$

$$\text{Encapsulation efficiency} = \frac{\text{Wt} - \text{Wf}}{\text{Wt}} \times 100 \quad (2)$$

where Wt is the total weight of drug fed, Wf is the weight of free drug in the supernatant, and Wnp is the weight of nanoparticles.

The concentration of free drug in the supernatant was quantified by measuring the absorbance at a wavelength of 259 nm via a ultraviolet-visible (UV-vis) spectrophotometer (PerkinElmer Lambda 35; Perkin Elmer). All the data were measured in triplicates and the result was expressed as a mean of three independent measurements. The analytical method was validated using a standard plot of ketoprofen lysinate in the range 1–4 μg/mL.

In vitro cytotoxicity study

hFOB 1.19 (ATCC® CRL11372™) cell line, derived from human fetal bone tissue, was purchased from American Type Culture Collection (ATCC, Manassas, VA, USA). The osteoblast SV40 large T antigen transfected cell line was grown in a base medium that comprised 1:1 mixture of Ham's F12 medium Dulbecco's modified Eagle's minimal essential medium with 2.5 mM lglutamine without phenol red. The complete growth medium for the cell line was prepared by adding fetal bovine serum to a final concentration of 10% and by supplementing with 0.3 mg/mL of Geneticin® selective antibiotic G418 (Sigma-Aldrich, St Louis, MO, USA) as recommended in the ATCC product sheet protocol.[53] The cultured cells were incubated at 34°C in an incubator supplied with 5% CO_2 in air atmosphere as described in the guideline procedures. The confluence of cells at approximately 80%–90% was used for seeding and further treatments.

Cell seeding and treatments

The human osteoblast cell line (hFOB1.19) was seeded into 96-well plates and incubated for 24–36 hours. Then, the cells were cocultured with surface-functionalized cockle shell–based calcium carbonate aragonite polymorph nanoparticles and those without surface functionalization at different concentrations (25, 50, 100, 200, 400, 800, and 1000 µg/mL) for 24 hours including wells for control. Likewise, different concentrations of ketoprofen lysinate, blank nanoparticles, and nanoparticle/drug complexes of both nanocarrier types were prepared and cocultured into each respective well at predetermined concentration levels of 15.625, 31.25, 62.5, 125, 250, 500, and 1000 µg/mL and incubated for 24 hour in cell culture incubator at 34°C.

MTT cell–based assay procedures

After incubation, all cultured media inside each well including the controls were aspirated, washed with PBS, and then replaced by 50 µL of fresh complete media prior to MTT treatment. Next, 10 µL of MTT reagent (Sigma-Aldrich) was added into each well including controls, and the plates were incubated for 4 hours at 34°C. Cultured medium inside all wells was removed properly and 150 µL of dimethyl sulfoxide was added to each well including the controls, and the samples were then gently shaken for 20 minutes in dark room. After that the sample compounds were quantified spectrophotometrically by a plate reader at a wavelength of 565 nm. The experiment was carried out in triplicates and the results were appropriately analyzed using Equation (3):.

$$\text{Cell viability (\%)} = \frac{\text{OD test}}{\text{OD control}} \times 100 \qquad (3)$$

where OD test is the optical density reading of the test result and OD control is the optical density reading of the control.

In vitro drug-release study

A total of 5 mg of nanocarrier/drug complex was suspended in 10 mL of PBS at pH 7.4 and pH 6.4. Then, the samples were gently and constantly rotated at 100 rpm in an incubator shaker (WiseCube; Wisd Laboratory Instruments) at 37°C. A total of 1 mL of the immersion liquid was taken out of the sample at predetermined intervals: every hour for the first 6 hours and followed by 24 hours for five consecutive days. An equal volume of the same buffer was then replaced in the sample. After that the liquid sample was centrifuged and the drug concentration was determined by measuring the absorbance at specific wavelength, λ_{max}=259, using a UV-vis spectrophotometer. The procedures were performed in triplicate for both types of nanocarrier/drug complexes.

Statistical analysis

Data analyses were performed using SPSS statistical analytic software (SPSS 14.0 for Windows; SPSS, Inc., Chicago, IL, USA). Independent *t*-test was used to find statistical differences between two means of both nanocarrier types. *p*-value <0.05 ($p<0.05$) was considered as statistical significance. All experiments were performed in triplicate unless otherwise indicated and the results were expressed as mean±standard deviation

Results and discussion

Size morphology, surface characterization, particle size distribution, and zeta potential

The size, shape, and surface characteristics of the surface-functionalized cockle shell–based calcium carbonate aragonite polymorph nanoparticles were analyzed by TEM and FESEM. Purification procedure proved that in general larger particles could be separated from whole nanoparticles. Figure 2A and B shows the transmission electron micrographs of cockle shell–based calcium carbonate aragonite nanoparticles without surface functionalization, before and after the purification process.

On the other hand, Figure 3A and B shows the micrographs of cockle shell–based calcium carbonate aragonite polymorph nanoparticles after surface functionalization before purification procedure at different magnifications. Meanwhile, Figure 3C is a transmission electron micrograph of the sample after purification procedure observed at a slightly higher magnification of 150,000×. These figures clearly present the significant effect of purification procedure on round-shaped cockle shell–based calcium carbonate aragonite polymorph nanoparticle samples, either before or after surface functionalization process during which larger-sized particles (more than 100 nm) are possibly filtered and removed through double filtration techniques during the purification process.

In addition, the huge difference in terms of nanoparticles' dispersion could also be compared between Figures 2 and 3. The distribution among cockle shell-based calcium carbonate aragonite polymorph nanoparticles was improved as the nanoparticles appeared more disperse to each other after the surface functionalization process, which is clearly shown in Figure 3A–C. Therefore, the synthesis method is

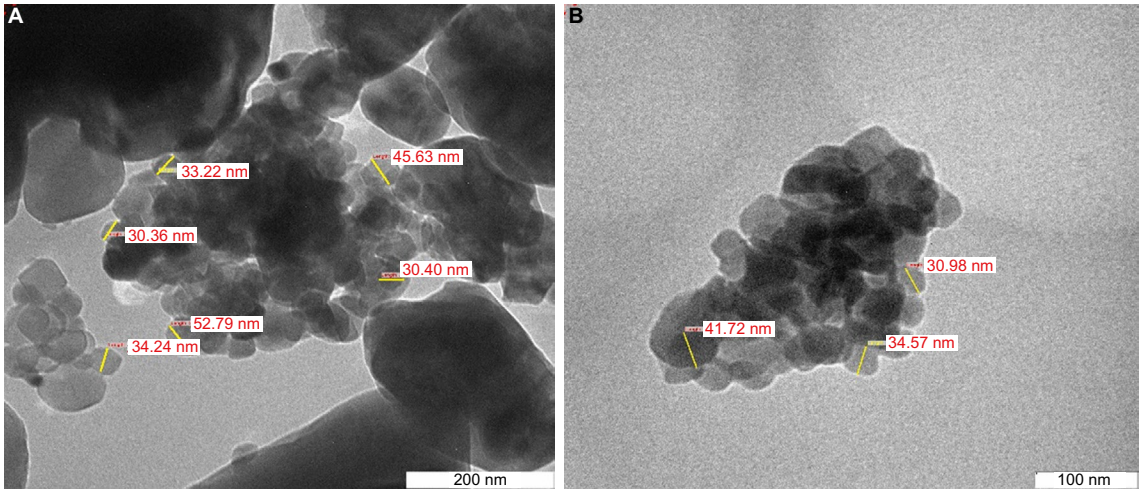

Figure 2 Transmission electron micrographs of cockle shell–based calcium carbonate aragonite polymorph nanoparticles without surface functionalization **(A)** before purification process and and **(B)** after purification process examined at 150,000× and 200,000× magnifications, respectively.

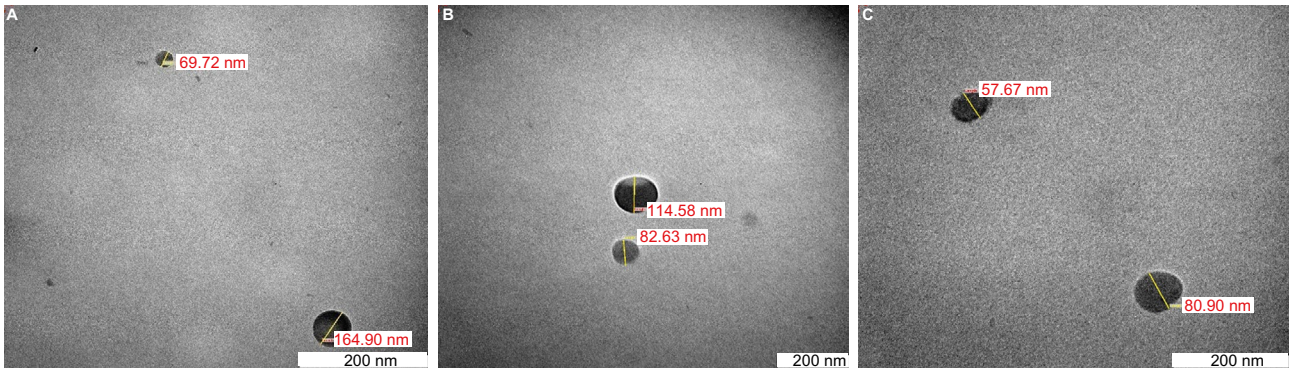

Figure 3 Transmission electron micrographs of surface-functionalized cockle shell–based calcium carbonate aragonite polymorph nanoparticles before purification procedure viewed at **(A)** 70,000× **(B)** 100,000× magnifications, and after purification procedure viewed at **(C)** 150,000× magnification.

advantageous for drug-delivery applications as for most of the time the presence of larger particles in the nanoparticle sample can interfere and give different experimental results in vitro.[54] Moreover, prevention of coarse agglomeration between nanoparticles by surface modification technique improves the overall distribution of nanoparticles, thereby increasing the biological effect during in vitro investigation in particular.[2,9,54]

On the other hand, Figure 4A and B is the micrographs of surface-functionalized cockle shell–based calcium carbonate nanoparticles before purification viewed at several magnifications, whereas Figure 5 is a micrograph

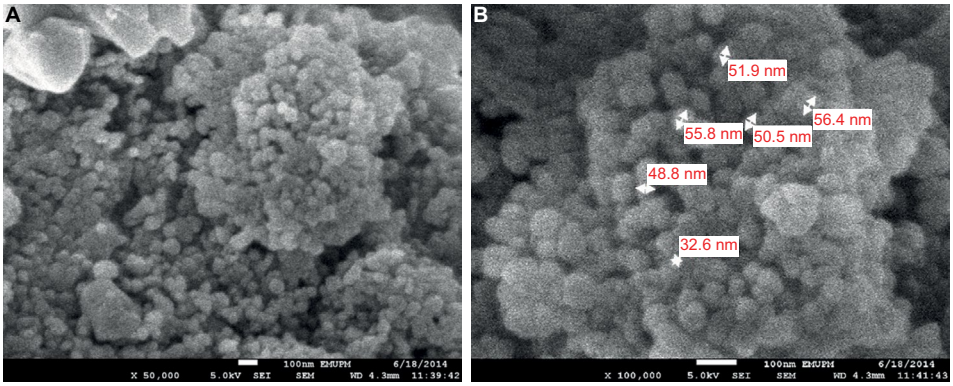

Figure 4 Field emission scanning electron micrographs of surface-functionalized cockle shell–based calcium carbonate aragonite polymorph nanoparticles viewed at different magnifications: **(A)** 50,000× and **(B)** 100,000×.

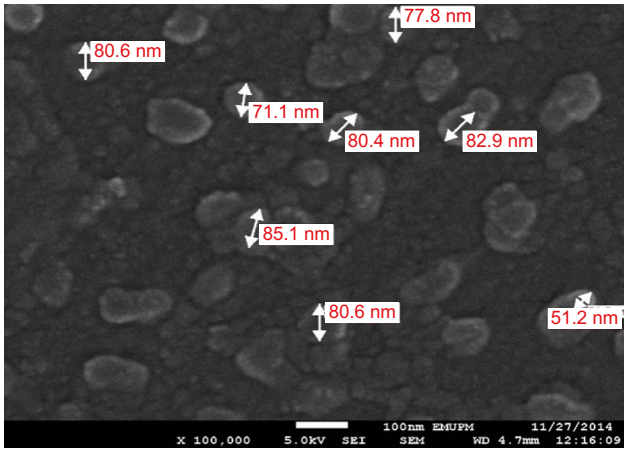

Figure 5 Field emission scanning electron micrograph of surface-functionalized cockle shell–based calcium carbonate aragonite spherical nanoparticles after filtration viewed at 100,000× magnification.

of those nanoparticles after filtration viewed at 100,000× magnification. The figure shows that the surfaces of these nanoparticles are rough and irregular rather than smooth and rigid, which reveals their porous nature. In addition, Figure 5 also ensures that the size range of most nanoparticles is less than 100 nm, which was confirmed by filtration method. Furthermore, the size of the largest nanoparticles viewed in the micrograph was only around 70–80 nm in diameter, after being purified.

Figure 6A shows the micrographs of the drug-loaded surface-functionalized cockle shell–based calcium carbonate aragonite polymorph nanoparticle (CSD) viewed at 100,000× magnification, whereas Figure 6B shows the micrographs of drug-loaded cockle shell–based calcium carbonate aragonite polymorph nanoparticle without surface functionalization (CXSD) at 150,000× magnification . The figures show that the size of the nanocarriers did not change even after the drug-loading process; this emphasizes that the drug molecules might have been possibly confined into pore channels of both porous cockle shell-based calcium carbonate nanoparticles during the physical encapsulation process of the drugs. Apart from that, Figure 6A also clearly reveals that surface functionalization could result in better size distribution among CSD complexes compared to CXSD sample as seen in Figure 6B. The aim of our research was to provide better prospective on surface-functionalized colloidal cockle shell–based calcium carbonate nanocarrier, which potentially lowers the risk of agglomeration among the nanoparticles that may affect their function and stability as an efficient drug carrier.

Moreover, the size distribution of the nanoparticles before and after the purification procedure based on the scattering intensity from the zetasizer analysis are shown in Figure 7A and B. The highest peaks in Figure 7A and B refer to the mode of particle size distributions which represents the size of the nanoparticles that are most commonly found in the surface-functionalized cockle shell-based calcium carbonate aragonite sample in deionized water. From the graphs, the sample after the purification procedure displays one prominent peak when compared to the sample before the purification procedure which portrays two distinct peaks, hence indicating that the purification procedure improved the consistency of the particle size distribution as shown in Figure 7A and B, respectively.

Besides, purified nanoparticles (Figure 7B) showed a narrower range of particle size distribution compared to nonpurified nanopaticles (Figure 7A). This shows that purification

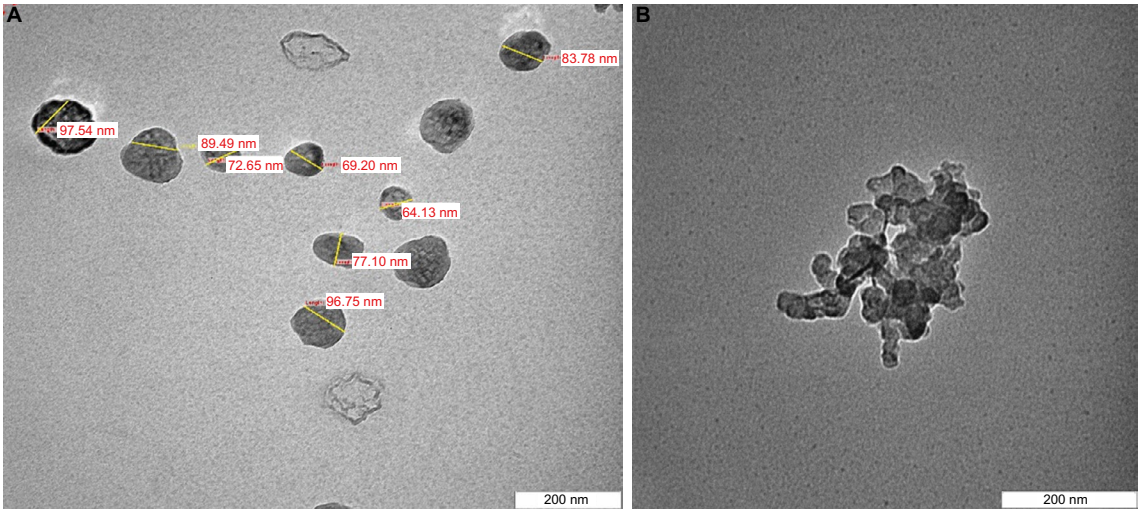

Figure 6 Transmission electron micrographs of **(A)** drug-loaded surface-functionalized cockle shell–based calcium carbonate aragonite polymorph nanocarrier and **(B)** drug-loaded cockle shell–based calcium carbonate aragonite polymorph nanocarrier without surface functionalization viewed at 100,000× and 150,000× magnifications, respectively.

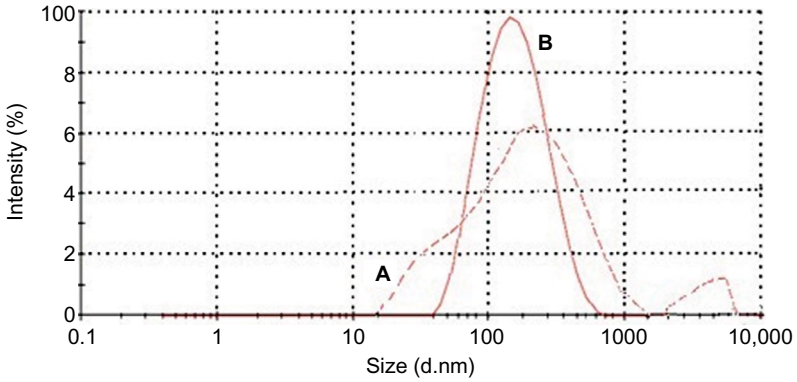

Figure 7 Size distributions based on scattering intensity (%) against diameter size of surface-functionalized cockle shell-based calcium carbonate aragonite nanoparticles (**A**) before and (**B**) after purification procedure

process had a significant effect on the size of nanoparticles; larger nanoparticles were filtered from the whole sample, which resulted in a better uniform size distribution. In addition, the results obtained agreed well with those obtained by TEM shown in Figure 2A. In fact, it was very important to exclude or filter larger nanoparticles from the whole sample as they might lead to coarse agglomeration, which could probably exert different effects toward biological systems.[54] Therefore, the suggested method is very advantageous in refining the size distribution of nanoparticle samples, especially for drug-delivery purpose.

Zeta potential is also one of the important parameters that characterize the surface property of the particles, especially for improving cellular interactions in drug-delivery system.[9–11] Table 1 displays zeta potential values of both cockle shell–based calcium carbonate nanoparticles without surface modification and surface-functionalized cockle shell–based calcium carbonate nanoparticles based on three replicate experimental measurements. The zeta potential of cockle shell–based calcium carbonate nanoparticle without surface modification was approximately calculated as 9.4 mV at pH 8.35. Yet surface functionalization was proved to enhance zeta potentials up to around 28.9 mV at pH 7.85, thereby resulting in more stable dispersion of the cockle shell–based calcium carbonate nanoparticles in suspension.

Table 1 Zeta potentials of cockle shell–based calcium carbonate nanoparticle without surface functionalization and surface-functionalized cockle shell–based calcium carbonate nanoparticles

Samples	Zeta potentials (mV) (mean ± SD)	pH measurements (mean ± SD)
Cockle shell–based calcium carbonate nanoparticle without surface functionalization	−9.4±0.8	8.35±0.01
Surface-functionalized cockle shell–based calcium carbonate nanoparticle	−28.9±0.1	7.85±0.01

Note: All samples showed statistically significant difference at $p<0.05$.
Abbreviation: SD, standard deviation.

As often reported in the literature, the desirable zeta potential value should be approximately ±30 mV so that sufficient surface charge can allow stable dispersion among particles in suspension, thereby preventing particles' aggregation.[9–11] The zeta potential of surface-functionalized cockle shell-based calcium carbonate nanoparticles is closer to the optimum zeta potential for drug delivery, hence allowing better stability and dispersion of the nanoparticles in suspension compared to the cockle shell-based calcium carbonate nanoparticle without surface modification. In fact, zeta potential value of surface-functionalized cockle shell–based calcium carbonate nanoparticles was found to be significantly higher compared to zeta potentials of those nanoparticles without surface modification, when statistically tested at $p<0.05$.

This finding further justifies the results obtained by TEM (Figures 2 and 3) regarding the visibly improved distribution and dispersion of the surface-functionalized cockle shell–based calcium carbonate nanoparticles sample compared to those without surface modification. Meanwhile, the sign of zeta potentials was found to be negative for both calcium carbonate samples. In addition, surface functionalization has also been found to influence the pH values of the samples. The pH of surface-functionalized cockle shell–based calcium carbonate nanoparticles was lower and more close to neutral pH, that is pH 7.85, whereas the pH of the sample before surface modification was 8.35. Therefore, this implies that calcium ions are adsorbed successfully onto the surface of the nanoparticles after surface functionalization process.

Drug-loading and encapsulation efficiencies

Drug-loading process was performed by incubating nanocarriers into concentrated drug solutions for a specific time period. Ketoprofen lysinate was selected as a model drug to demonstrate the loading ability of the surface-functionalized cockle shell–based calcium carbonate aragonite nanoparticles as a drug carrier. Various ratios of nanocarrier to drug were tested in order to obtain a best formulation for loading process as shown in Figure 8. At a ratio of 5:1, CSD showed a highest percentage of encapsulation efficiency (89.9%) but a lowest percentage of (17.9%) loading capacity. Similarly, at a ratio of 5:1, CXSD also showed a highest percentage of encapsulation efficiency but a lowest percentage of drug-loading capacity (15.9%). A similar trend of findings was also reported by others.[8,55]

In general, increased drug concentrations during loading process resulted in increased percentage of drug loading; this could also increase the amount of drug compounds lost to the surrounding medium due to lesser effectiveness of nanocarriers to load most of the drug compounds. The results of our study emphasize that highest encapsulation efficiency was observed at a nanoparticle:drug ratio of 5:1 for both types of nanocarriers. For instance, while loading 5 mg of surface-functionalized cockle shell–based calcium carbonate aragonite nanoparticles with 1 mg of ketoprofen lysinate, about 89.9% of ketoprofen lysinate was adsorbed onto the surface of the nanoparticles and based on the loading content, 17.9% of the nanoparticles was being loaded by the drug compound. Hence, in general, the concentration of drugs plays a significant role in determining both the encapsulation efficiency and drug-loading capacity of the nanocarrier/drug complexes during the loading process.

In general, both encapsulation and drug-loading efficiencies of the CSD complex were higher compared to the CXSD complex at all formulated nanoparticle/drug ratios as shown in Figure 8A and B, respectively. Indeed, the percentages of encapsulation and drug-loading efficiencies of the CSD sample were significantly proven to be higher compared to those of CXSD sample, which was statistically analyzed at $p<0.05$ for all nanoparticle/drug formulated ratios. These results show the substantial effect of surface functionalization in enhancing the ability of cockle shell–based calcium carbonate aragonite nanocarrier to load more drugs during loading process. In our opinion, surface functionalization increases the driving forces, especially the electrostatic attractions, between the nanoparticles and drug molecules, thereby resulting in higher encapsulation efficiency and tolerable percentage of drug-loading capacity. Besides, surface modification based on ionic interactions between the CSD sample and drug molecules might also improve transfection process during loading procedure effectively.[9–11]

X-ray diffraction (XRD)

The crystalline nature of materials in all the samples after the loading process was analyzed by XRD. Figures 9 and 10 show the strong and intact crystallization state of all the samples in corresponding XRD patterns. The aragonite phase of the samples was confirmed according to JCPDS file no. 00-041-1475. The XRD patterns of all the cockle shell–based calcium carbonate samples before and after loading of both nanocarrier types indicate that the aragonite crystalline phase of the samples did not change or alter after

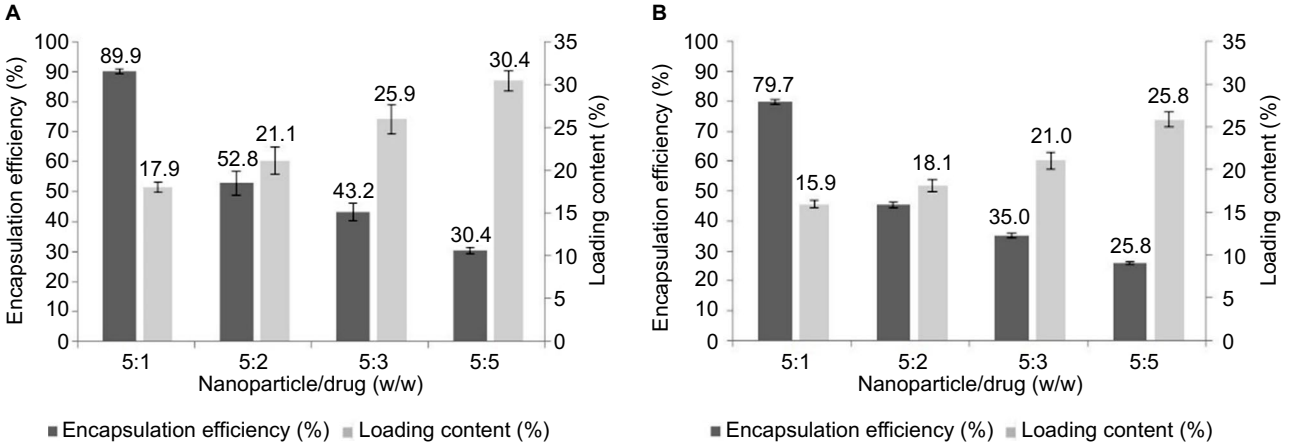

Figure 8 Percentages of encapsulation efficiency and loading capacity of **(A)** surface-functionalized cockle shell–based calcium carbonate aragonite nanoparticle/drug complex and **(B)** cockle shell–based calcium carbonate aragonite nanoparticle without surface modification/drug complex, based on various loading ratios.

Notes: The percentages of both encapsulation efficiency and drug-loading capacity of nanoparticle/drug complex sample (A) were significantly higher than the sample (B) at all formulated ratios statistically tested at $p<0.05$.

being loaded with the drugs (Figures 9B, C and 10B, C). The original phase of calcium carbonate aragonite crystal remained same, although it underwent the whole formulation process. Furthermore, these comparable patterns of XRD patterns also demonstrate that the drug molecule was loaded within the nanocarriers. Similar patterns of findings were also observed by other studies.[8,21,56,57]

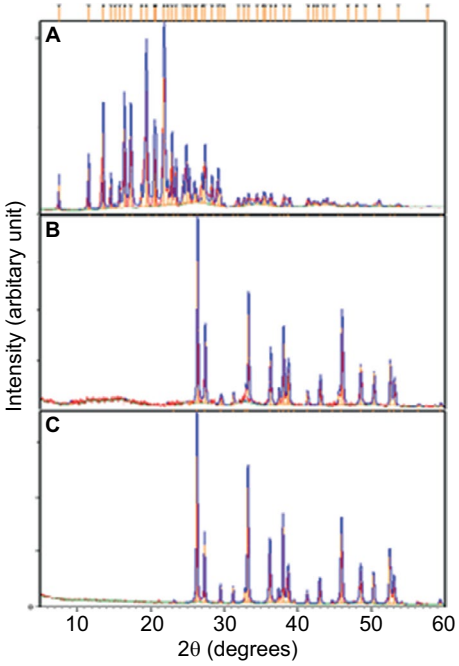

Figure 9 Comparison of X-ray diffraction patterns of **(A)** ketofropen lysinate drug, **(B)** drug-loaded surface-functionalized cockle shell–based calcium carbonate aragonite nanoparticles, and **(C)** blank surface-functionalized cockle shell–based calcium carbonate aragonite nanocarrier.

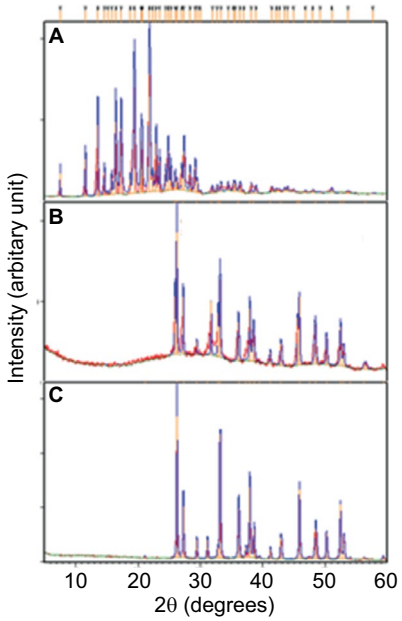

Figure 10 X-ray diffraction patterns of **(A)** ketofropen lysinate drug, **(B)** drug-loaded cockle shell–based calcium carbonate aragonite nanoparticles without surface modification nanoparticles, and **(C)** blank cockle shell–based calcium carbonate aragonite without surface modification nanocarrier.

FTIR

The FTIR spectra of ketoprofen lysinate, CXSD, and CSD are presented in Figure 11A–C, respectively. The FTIR bands of CXSD at 1780 cm^{-1} and of CSD at 1786 cm^{-1} are due to C=O stretching vibration. Bands of CXSD at 1780 cm^{-1}, 1451 cm^{-1}, 1082 cm^{-1}, 854 cm^{-1}, and 700 cm^{-1} and of CSD at 1786 cm^{-1}, 1458 cm^{-1}, 1083 cm^{-1}, 856 cm^{-1}, and 707 cm^{-1} were descriptive FTIR absorption bands of carbonate groups that are typically found in aragonite polymorph calcium carbonate.[34,36,39] The presence of these prominent FTIR bands of aragonite polymorph calcium carbonate in the samples (Figure 11B and C) indicates that the aragonite polymorphism of both nanocarriers remained the same after the drug loading process.

Additionally, another three prominent FTIR bands of CXSD were also observed at 3386 cm^{-1}, 1020 cm^{-1}, and 559 cm^{1} and of CSD at 3398 cm^{-1}, 1025 cm^{-1}, and 565 cm^{-1}. The bands at 3386 cm^{-1} and 3398 cm^{-1} were assigned as -–NH stretch. In the FTIR fingerprint region, there were –CN stretching band appeared at 1020 cm^{-1} and 1025 cm^{-1} and –CH bending vibration at 559 cm^{-1} and 565 cm^{-1} in both samples. The appearance of –NH stretching, –CN stretching and –CH bending bands are possibly due to the characteristic bands of the ketoprofen lysinate drug. The presence of nitrogen (N) element from the amine group and the hydrogen (H) from the alkane group in both the calcium carbonate nanocarrier-drug complexes are potentially contributed by the drug component, considering that the elemental compositions in both types of calcium carbonate nanocarriers should only contain carbon (C), oxygen (O), and calcium (Ca) elements. This result, therefore, implies that ketoprofen lysinate has been successfully adsorbed into both types of nanocarriers.

In addition, the FTIR results shown in Figure 11 also demonstrates that the interactions between the drug and both of the nanocarriers are due to weak intermolecular van der Waals forces such as hydrogen bonding, dipole–dipole attraction, and electrostatic attraction. The observation of a strong absorption band at around 3386 cm^{-1} and 3398 cm^{-1} for CXSD and CSD, respectively, shows that the formation of hydrogen bond between the drug and the nanocarrier cannot be ruled out. Furthermore, comparison of the FTIR absorption spectra between both nanocarriers and the drug also indicates that CSD had relatively stronger bond than CXSD, as most of their FTIR absorption spectra appeared at comparatively higher vibrational wavenumbers.

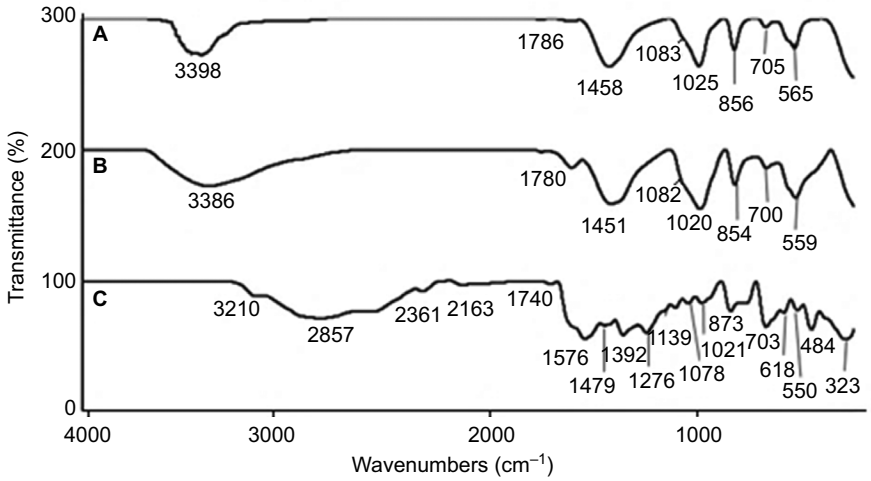

Figure 11 FTIR spectra of **(A)** ketoprofen lysinate drug, **(B)** drug-loaded cockle shell–based calcium carbonate aragonite nanoparticles without surface modification, and **(C)** drug-loaded surface-functionalized cockle shell–based calcium carbonate aragonite nanoparticles.

MTT cytotoxicity assay

In vitro cytotoxicity analysis of blank surface-functionalized cockle shell–based calcium carbonate aragonite and those samples without surface modification shows a good biocompatibility based on cell viability after 24 hours of incubation (Figure 12). However, the cell viability percentage based on controlled cells of the blank samples of surface-functionalized samples was higher compared to those without surface modification, which was ~79.5% at 1000 μg/mL.

The result demonstrates that the surface modification of cockle shell–based calcium carbonate aragonite nanoparticles could apparently improve the toxic effect of the nanoparticle sample prepared using BS-12 surfactant. Hence, this situation enhances the percentage of cell viability up to ±90% even at high concentration of 1000 μg/mL. Therefore, this work suggests that surface-functionalized cockle shell–based calcium carbonate aragonite nanoparticle is potentially a better material in terms of its reliably low cytotoxic effect on biological cells and is safe for use in many biomedical applications, including its use as a biocompatible carrier agent in drug-delivery system.

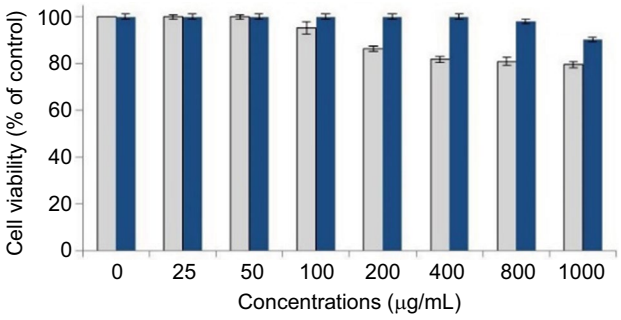

Figure 12 In vitro cytotoxicity study of blank surface-functionalized cockle shell–based calcium carbonate aragonite (blue bars) and cockle shell–based calcium carbonate aragonite without surface modification nanoparticles (gray bars) on human fetal bone tissue cell line (hFOB1.19) at different concentrations during 24 hours of incubation.
Note: The statistical analysis showed that the cell viability of surface-functionalized cockle shell-based calcium carbonate aragonite nanoparticle samples was significantly higher compared to cockle shell-based calcium carbonate aragonite nanoparticles without surface modification only at 100 until 1000 μg/mL. However, at concentrations below 100 μg/mL, both type of nanocarriers have similar cell viability percentage which is 100%. Cell viability for surface-functionalized [blue bar] at concentration: 0: 100%; 25: 100%; 50: 100%; 100: 100%; 200: 100%; 400: 99.8%; 800: 98.2%; 1000: 90.1%. Cell viability for cockle shell-based $CaCO_3$ without surface modification [gray bars] at concentration; 0: 100%; 25: 100%; 50: 100%; 100: 95.3%; 200: 86.3%; 400: 81.7%; 800: 80.9%; 1000: 79.5%.

Figure 13A and B shows the cytotoxic effect of free ketoprofen lysinate drug compared to similar concentrations of CSD and CXSD complexes on human fetal bone tissue cell lines (hFOB1.19) at different concentrations during 24 hours of incubation. In general, when ketoprofen lysinate drug concentrations were doubly reduced, the cell viability percentages increased, which indicates a decrease in the cytotoxic effect of the drug during 24 hours of incubation period (Figure 13A and B). Similar result of drug toxicity study[58] that employed different cell lines was also reported.

Cytotoxicity analysis reveals that ketoprofen lysinate–free drug was moderately toxic when directly exposed to human fetal bone tissue cell lines, which approximately showed 63% of cell viability at high concentration of 1000 μg/mL during 24 hours of incubation. However, the toxic effect of pure ketoprofen lysinate drug on the cell lines could be improved by loading the drug components either onto the surface-functionalized cockle shell–based calcium carbonate aragonite or onto those nanoparticles without surface modification, prepared at similar drug concentrations.

Reduced drug toxicity observed might be probably due to the sustained release effect of the drugs during 24 hours of incubation. These results demonstrate that both nanocarrier types could apparently reduce the toxicity profile of a pure

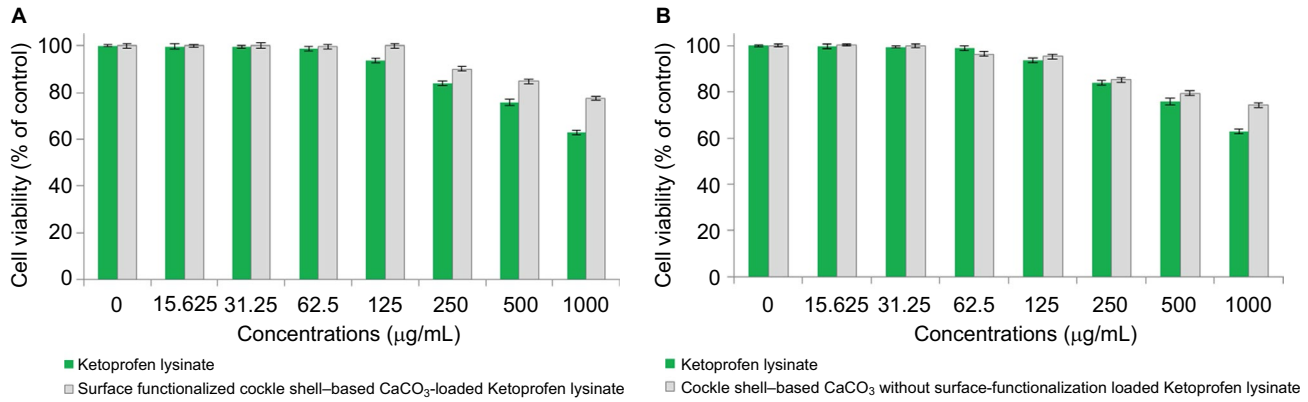

Figure 13 In vitro cytotoxicity studies on the human fetal bone tissue cell lines (hFOB 1.19) exposed to ketoprofen lysinate free drug along with **(A)** drug-loaded surface-functionalized cockle shell–based calcium carbonate aragonite nanoparticle and **(B)** drug-loaded cockle shell–based calcium carbonate aragonite nanoparticle without surface modification at several concentrations during 24 hours of incubation period.

drug by loading it onto either type of the nanocarriers. Similar to the features of other drug carriers, this special feature of cockle shell–based materials emphasize that they possess considerable potential as drug carriers, which can possibly slow down or prevent the undesired direct toxic effects of drugs on biological cells, a characteristic feature which is beneficial for delivery system.

In addition, cytotoxicity analysis indicates that the CSD sample generally had a higher percentage of cell viability compared to CXSD, nearly at all concentrations. For example, the CSD complex achieved almost 100% of cell viability based on controlled cells at a concentration of 125 μg/mL. On the other hand, CXSD had a slightly lower percentage of cell viability (comparatively 95% at 24 hours of incubation). Therefore, MTT cell viability study suggests that surface functionalization of the cockle shell–based calcium carbonate aragonite nanoparticles can enhance the biological cell viability and reduce cytotoxic effects of the calcium carbonate aragonite–derived cockle shell biomaterial, thereby possibly improving their cellular interactions within the biological systems in particular.

Drug release kinetics

Drug release kinetic was conducted at two different pH environments. It is well known that the pH at inflammation site is slightly lower[59–61] than the normal physiological pH, which is around 7.4. In this study, we chose PBS whose pH was 6.4 as dissolution medium to investigate the release kinetic of both nanocarrier types simulated at comparable pH of the inflammatory tissues. The in vitro release profiles of ketoprofen lysinate from the CSD and CXSD complexes at respective pH 7.4 and pH 6.4 are shown in Figures 14 and 15.

At pH 7.4, almost 97% of ketoprofen lysinate was released from the CXSD complex in 24 hours, whereas ~70% of the lysinate of the drug component was released from the CSD complex in 24 hours. The difference in the release rate of both nanoparticle/drug complexes thus suggests that the CSD sample shows higher possibility of sustained release characteristic than the CXSD complex at normal physiological pH.

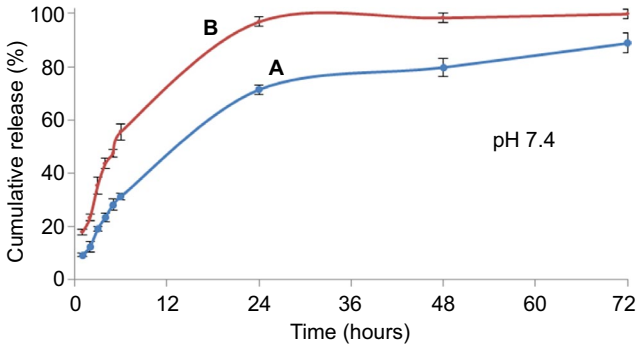

Figure 14 In vitro release profile of ketoprofen lysinate from **(A)** drug-loaded surface-functionalized cockle shell–based calcium carbonate aragonite nanoparticles and **(B)** drug-loaded cockle shell–based calcium carbonate aragonite without surface modification nanoparticles at pH 7.4 in phosphate buffered saline.
Note: The cumulative release percentages at pH 7.4 of the sample (B) were significantly higher than the sample (A) when statistically tested at $p<0.05$.

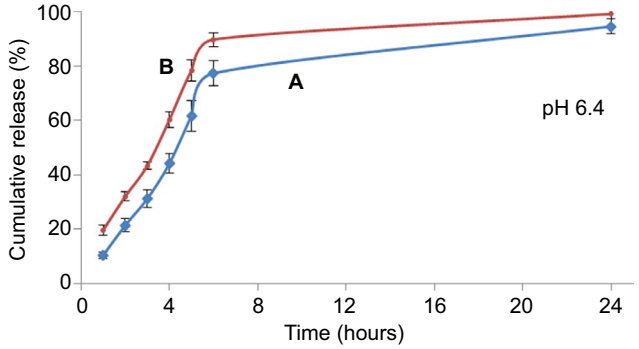

Figure 15 In vitro release profile of ketoprofen lysinate from **(A)** drug-loaded surface-functionalized cockle shell–based calcium carbonate aragonite nanoparticles and **(B)** drug-loaded cockle shell–based calcium carbonate aragonite nanoparticles without surface modification at pH 6.4 in phosphate buffered saline.
Note: The cumulative release percentages at pH 6.4 of the sample (A) were significantly higher than the sample (B) tested statistically at $p<0.05$.

In addition, CXSD complex initially released 55% of ketoprofen lysinate within 6 hours at pH 7.4. Conversely, the CSD complex released ~30% of ketoprofen lysinate within 6 hours period followed by a gradual unloading process of up to 90% after 72 hours (Figure 14). A higher cumulative release percentage by the CXSD sample was observed compared to the CSD sample, which was statistically significant at $p<0.05$. These findings show that the surface modification of cockle shell–based calcium carbonate aragonite nanoparticles might apparently assuage the initial burst release, thereby resulting in a controlled release rate of the whole dissolution process during 72 hours at pH 7.4 in vitro.

Figure 15 displays the in vitro release profiles of ketoprofen lysinate drug from both types of nanoparticle/drug complexes at pH 6.4 in PBS. In general, the cumulative release percentages of the CXSD complex at pH 6.4 were higher compared to that of the CSD complex, . which was statistically significant at $p<0.05$. The lower dissolution percentages of the CSD complex thus suggest that surface functionalization is also capable of controlling drug release profiles even at acidic environments. Therefore, it slows down the 24 hours release rate of ketoprofen lysinate drug from the nanoparticle/drug complex.

In general, the results of the dissolution studies are similar to those reported by other drug-delivery studies.[8,23,62] Likewise, a slightly acidic environment expedited the release kinetic compared to normal physiological pH. Figures 14 and 15 show that both types of nanoparticle/drug complexes had a significantly higher release rate in slightly acidic medium (pH 6.4) compared to the pH of the surrounding medium (pH 7.4). The release percentages of the CSD complex at pH 6.4 were cumulatively more than 90% in 24 hours, whereas at pH 7.4, the percentages of similar nanoparticle/drug complex remained at ~90% even at 72 hours, which helped in retaining its drug encapsulation ability. Comparably, the release percentage of the CXSD complex within 6 hours was higher at pH 6.4 (almost 90%) compared to that at pH 7.4 (55%) as shown in Figures 14 and 15, respectively.

The release profiles, therefore, indicate that both cockle shell-based calcium carbonate aragonite loaded drug complexes are sensitive to pH changes as they would release more drug compounds in acidic environment compared to normal physiological pH. Moreover, the results obtained in this study on the pH-sensitive characteristic of similar type of cockle shell–based calcium carbonate material and use of different methods of nanoparticle preparation for drug delivery are in good agreement with previously reported finding.[22] In fact, excellent pH-sensitive characteristics of both cockle shell–based calcium carbonate aragonite drug carrier types are very advantageous for drug-delivery system, as the drug compounds might be delivered only toward a desired site of action without affecting other healthy tissues in the body.

In our opinion, increased release of drug components from their nanocarriers in a more acidic environment might also be possibly due to the gradual dissolution of materials during release process. Furthermore, control of dissolution rate under physiological condition while selectively enhancing the release process in response to pH changes at a specific location also implied that this type of delivery agents might have more tendency to achieve high therapeutic concentrations at targeted location such as the inflammation site, thereby possibly improving therapeutic effectiveness specifically at affected areas.

Conclusion

This work focused on the development, characterization, and evaluation of surface-functionalized cockle shell–based calcium carbonate aragonite polymorph nanoparticles as a carrier agent for drug-delivery colloidal system. The study further justifies the utilization of newly emerging type of calcium carbonate sources derived from cockle shells that contains purely aragonite polymorph; this represents a safer biomaterial for drug-delivery applications after surface modification. Functionalization process improved the surface properties of the resulting nanoparticles and at the same time successfully produced nanoparticles with high homogeneity in sizes and morphologies. This effectively enhanced optimal zeta potentials, thereby increasing the dispersion and stability of the nanoparticles in colloidal suspension. In addition, the purification process made the nanoparticle synthesis method superior by producing refined nanoparticles within promising size range of less than 100 nanometers, a feature favorable for drug-delivery purposes. Surface functionalization process also increased the toxic level of nanoparticles on biological cells, thus validating its potential ability as a safe biocompatible material applicable for biomedical utilizations. In fact, the modified synthesis process did not only improve the efficiency of drug delivery but also concomitantly improved both the quality and safety profiles of the drugs and the nanocarrier for delivery system. Although it is impossible to exactly mimic natural conditions during drug-delivery studies, in vitro studies of both drug loading and release profiles of the surface-functionalized cockle shell–based calcium carbonate aragonite polymorph nanoparticles emphasize that these nanoparticles possess excellent characteristics to be practically used as pH-sensitive nanocarrier devices; therefore, they

possess better drug-delivering capacity and have a potential to be used in advanced drug-delivery systems in the near future.

Author contributions

All authors contributed toward data analysis, drafting and critically revising the paper and agree to be accountable for all aspects of the work.

Disclosure

The authors report no conflicts of interest in this work.

References

1. Sahoo SK, Parveen S, Panda JJ. The present and future of nanotechnology in human health care. *Nanomedicine*. 2007;3(1):20–31.
2. Moghimi SM, Hunter AC, Murray JC. Nanomedicine: current status and future prospects. *FASEB J*. 2005;19(3):311–330.
3. Koo OM, Rubinstein I, Onyuksel H. Role of nanotechnology in targeted drug delivery and imaging: a concise review. *Nanomedicine*. 2005;1(3):193–212.
4. Mishra B, Patel BB, Tiwari S. Colloidal nanocarriers: a review on formulation technology, types and applications toward targeted drug delivery. *Nanomedicine*. 2010;6(1):9–24.
5. Parveen S, Misra R, Sahoo SK. Nanoparticles: a boon to drug delivery, therapeutics, diagnostics and imaging. *Nanomedicine*. 2012;8(2):147–166.
6. Newcomb RW. *Nanotechnology for Biomedicine: Past, Present and Future. Proceedings of the Second International Conference on Pervasive Technologies Related to Assistive Environments, Petra'09. Article no. 69*, *9–13 June 2009*. Corfu, Greece: ACM.
7. Faraji AH, Wipf P. Nanoparticles in cellular drug delivery. *Bioorg Med Chem*. 2009;17(8):2950–2962.
8. Kamba SA, Ismail M, Hussein-Al-Ali SH, Ibrahim TA, Zakaria ZA. In vitro delivery and controlled release of Doxorubicin for targeting osteosarcoma bone cancer. *Molecules*. 2013;18(9):10580–10598.
9. Xu ZP, Zeng QH, Lu GQ, Yu AB. Inorganic nanoparticles as carriers for efficient cellular delivery. *Chem Eng Sci*. 2006;61(3):1027–1040.
10. Singh R, Lillard JW Jr. Nanoparticle-based targeted drug delivery. *Exp Mol Pathol*. 2009;86(3):215–223.
11. Mohanraj VJ, Chen Y. Nanoparticles – a review. *Trop J Pharm Res*. 2006;5(1):561–573.
12. Ueno Y, Futagawa H, Takagi Y, Ueno A, Mizushima Y. Drug-incorporating calcium carbonate nanoparticles for a new delivery system. *J Control Release*. 2005;103(1):93–98.
13. Kim SK, Foote MB, Huang L. Targeted delivery of EV peptide to tumor cell cytoplasm using lipid coated calcium carbonate nanoparticles. *Cancer Lett*. 2013;334(2):311–318.
14. Svenskaya Y, Parakhonskiy B, Haase A, et al. Anticancer drug delivery system based on calcium carbonate particles loaded with a photosensitizer. *Biophys Chem*. 2013;182:11–15.
15. Park JH, Saravanakumar G, Kim K, Kwon IC. Targeted delivery of low molecular drugs using chitosan and its derivatives. *Adv Drug Deliv Rev*. 2010;62(1):28–41.
16. Kumar A, Zhang X, Liang XJ. Gold nanoparticles: emerging paradigm for targeted drug delivery system. *Biotechnol Adv*. 2013;31(5):593–606.
17. Rai M, Yadav A, Gade A. Silver nanoparticles as a new generation of antimicrobials. *Biotechnol Adv*. 2009;27(1):76–83.
18. Prakash S, Malhotra M, Shao W, Tomaro-Duchesneau C, Abbasi S. Polymeric nanohybrids and functionalized carbon nanotubes as drug delivery carriers for cancer therapy. *Adv Drug Deliv Rev*. 2011;63(14–15):1340–1351.
19. Kievit FM, Wang FY, Fang C, et al. Doxorubicin loaded iron oxide nanoparticles overcome multidrug resistance in cancer in vitro. *J Control Release*. 2011;152(1):76–83.
20. Oyerokun FT, Vaia RA. Distribution in the grafting density of end-functionalized polymer chains adsorbed onto nanoparticle surfaces. *Macromolecules*. 2012;45(18):7649−7659.
21. Saidykhan L, Abu Bakar MZ, Rukayadi Y, Kura AU, Latifah SY. Development of nanoantibiotic delivery system using cockle shell-derived aragonite nanoparticles for treatment of osteomyelitis. *Int J Nanomedicine*. 2016;11:661–673.
22. Shafiu Kamba A, Ismail M, Tengku Ibrahim TA, Zakaria ZA. A pH-sensitive, biobased calcium carbonate aragonite nanocrystal as a novel anticancer delivery system. *Biomed Res Int*. 2013;2013:587451.
23. Zhao D, Liu CJ, Zhuo RX, Cheng SX. Alginate/$CaCO_3$ hybrid nanoparticles for efficient co-delivery of antitumor gene and drug. *Mol Pharm*. 2012;9(10):2887–2893.
24. Liang P, Zhao D, Wang CQ, Zong JY, Zhuo RX, Cheng SX. Facile preparation of heparin/$CaCO_3$/CaP hybrid nano-carriers with controllable size for anticancer drug delivery. *Colloids Surf B Biointerfaces*. 2013;102:783–788.
25. Yu J, Lei M, Cheng B. Facile preparation of monodispersed calcium carbonate spherical particles via a simple precipitation reaction. *Mater Chem Phys*. 2004;88(1):1–4.
26. Yu J, Lei M, Cheng B, Zhao X. Facile preparation of calcium carbonate particles with unusual morphologies by precipitation reaction. *J Cryst Growth*. 2004;261(4):566–570.
27. Hu Z, Deng Y. Synthesis of needle-like aragonite from calcium chloride and sparingly soluble magnesium carbonate. *Powder Technol*. 2004;140(1–2):10–16.
28. Yan G, Wang L, Huang J. The crystallization behavior of calcium carbonate in ethanol/water solution containing mixed nonionic/anionic surfactants. *Powder Technol*. 2009;192(1):58–64.
29. Chang MC, Tai CY. Effect of the magnetic field on the growth rate of aragonite and the precipitation of $CaCO_3$. *Chem Eng J*. 2010;164(1):1–9.
30. Tran HV, Tran LD, Vu HD, Thai. Facile surface modification of nano-precipitated calcium carbonate by adsorption of sodium stearate in aqueous solution. *Colloids Surf A*. 2010;366(1–3):95–103.
31. Choi KM, Kuroda K. Polymorph control of calcium carbonate on the surface of mesoporous silica. *Cryst Growth Des*. 2012;12(2):887−893.
32. Sargheini J, Ataie A, Salili SM, Hoseinion AA. One-step facile synthesis of $CaCO_3$ nanoparticles via mechano-chemical route. *Powder Technol*. 2012;219:72–77.
33. Koga N, Kasahara D, Kimura T. Aragonite crystal growth and solid-state aragonite–calcite transformation: a physico–geometrical relationship via thermal dehydration of included water. *Cryst Growth Des*. 2013;13(5):2238–2246.
34. Kamba AS, Ismail M, Ibrahim TA, Zakaria ZA. Synthesis and characterisation of calcium carbonate aragonite nanocrystals from cockle shell powder (*Anadara granosa*). *J Nanomater*. 2013;2013:1–9.
35. Bakar ZA, Hussein BF, Mustapha NM. Cockle shell-based biocomposite scaffold for bone tissue engineering. In: Eberli D, editor. *Regenerative Medicine and Tissue Engineering – Cells and Biomaterials*. Rijeka, Croatia: InTech; 2011:365–390.
36. Bharatham H, Zakaria MZ, Perimal EK, Yusof LM, Hamid M. Mineral and physiochemical evaluation of cockle shell (anadara granosa) and other selected molluscan shell as potential biomaterials. *Sains Malaysiana*. 2014;43(7):1023–1029.
37. Stupp SI, Braun PV. Molecular manipulation of microstructures biomaterials, ceramics and semiconductors. *Science*. 1997;277(5330):1242–1248.
38. Wang C, Zhao J, Zhao X, Bala H, Wang Z. Synthesis of nanosized calcium carbonate (aragonite) via a polyacrylamide inducing process. *Powder Technol*. 2006;163(3):134–138.
39. Islam KN, Zuki AB, Ali ME, et al. Facile synthesis of calcium carbonate nanoparticles from cockle shells. *J Nanomater*. 2012;2012:5.
40. Zakaria ZAB, Zakaria N, Kasim Z. Mineral composition of the cockle (*Anadara granosa*) shells, hard clamp (*Meretrix meretrix*) shells and corals (Porites. spp): a comparative study. *J Anim Vet Adv*. 2004;3(7):445–447.

41. Awang-Hazmi AJ, Zuki ABZ, Noordin MM, Jalila A, Norimah Y. Mineral composition of the cockle (*Anadara granosa*) shells of west coast of peninsular Malaysia and its potential as biomaterial for use in bone repair. *J Anim Vet Adv*. 2007;6(5):591–594.
42. Li G, Li Z, Ma H. Synthesis of aragonite by carbonization from dolomite without any additives. *Int J Miner Process*. 2013;123:25–31.
43. Hu Z, Shao M, Cai Q, et al. Synthesis of needle-like aragonite from limestone in the presence of magnesium chloride. *J Mater Process Technol*. 2009;209(3):1607–1611.
44. Marchac D, Sandor G. Use of coral granules in the craniofacial skeleton. *J Craniofac Surg*. 1994;5(4):213–217.
45. Vuola J, Böhling T, Kinnunen J, Hirvensalo E, Asko-Seljavaara S. Natural coral as bone-defect-filling material. *J Biomed Mater Res*. 2000;51(1):117–122.
46. Islam KN, Bakar MZ, Ali ME, et al. A novel method for the synthesis of calcium carbonate (aragonite) nanoparticles from cockle shells. *Powder Technol*. 2013;235:70–75.
47. Huang YC, Fowkes FM, Lloyd TB, Sanders ND. Adsorption of calcium ions from calcium chloride solutions onto calcium carbonate particles. *Langmuir*. 1991;7(8):1742–1748.
48. Plank J, Bassioni G. Adsorption of carboxylate anions on a $CaCO_3$ surface. *Z. Naturforsch*. 2007;2007(62b):1277–1284.
49. Song MG, Kim JY, Kim JD. Effect of sodium stearate and calcium ion on dispersion properties of precipitated calcium carbonate suspensions. *Colloids Surf A Physicochem Eng Asp*. 2003;229(1–3):75–83.
50. El-Sheikh SM, El-Sherbiny S, Barhoum A, Deng Y. Effects of cationic surfactant during the precipitation of calcium carbonate nano-particles on their size, morphology and other characteristics. *Colloids Surf A Physicochem Eng Asp*. 2013;422:44–49.
51. Wang C, Liu Y, Bala H, et al. Facile preparation of $CaCO_3$ nanoparticles with self-dispersing properties in the presence of dodecyl dimethyl betaine. *Colloids Surf A Physicochem Eng Asp*. 2007;297(1–3):179–182.
52. Moulin P, Roques H. Zeta potential measurement of calcium carbonate. *J Colloid Interface Sci*. 2003;261:115–126.
53. American Type Culture Collection. *Product Sheet Guideline of hFOB 1.19 (ATCC® CRL11372 ™) Cell Line*. Manassas, VA: American Type Culture Collection; 2013:1–3.
54. Bihari P, Vippola M, Schultes S, et al. Optimized dispersion of nanoparticles for biological in vitro and in vivo studies. *Particle Fibre Toxicol*. 2008;5:14.
55. Ding M, Zhou L, Fu X, Tan H, Li J, Fu Q. Biodegradable gemini multiblock poly (ε-caprolactone urethane)s towards controllable micellization. *Soft Matter.* 2010;6:2087–2092.
56. Mello VAD, Ricci-Junior E. Encapsulation of naproxen in nanostructured system: structural characterization and in vitro release studies. *Quím Nova*. 2011;34(6):933–939.
57. Kalita S, Devi B, Kandimalla R, et al. Chloramphenicol encapsulated in poly-ε-caprolactone-pluronic composite: nanoparticles for treatment of MRSA-infected burn wounds. *Int J Nanomedicine*. 2015;10:2971–2984.
58. Stigliani M, Aquino RP, Del Gaudio P, Mencherini T, Sansone F, Russo P. Non-steroidal anti-inflammatory drug for pulmonary administration: design and investigation of ketoprofen lysinate fine dry powders. *Int J Pharm*. 2013;448(1):198–204.
59. Ueno T, Tsuchiya H, Mizogami M, Takakura K. Local anesthetic failure associated with inflammation: verification of the acidosis mechanism and the hypothetic participation of inflammatory peroxynitrite. *J Inflamm Res*. 2008;1:41–48.
60. Panyam J, Patil Y. Distribution: movement of drugs through the body. In: Cox S, editor. *Preclinical Development Handbook: ADME and Biopharmaceutical Properties*. Hoboken, NJ: Wiley-Interscience Publication; 2008:332.
61. Herath HM, Cabot PJ, Shaw PN, Hewavitharana AK. Study of beta endorphin metabolism in inflamed tissue, serum and trypsin solution by liquid chromatography-tandem mass spectrometric analysis. *Anal Bioanal Chem*. 2012;402(6):2089–2100.
62. Peng C, Zhao Q, Gao C. Sustained delivery of doxorubicin by porous $CaCO_3$ and chitosan/alginate multilayers-coated $CaCO_3$ microparticles. *Colloids Surf A Physicochem Eng Asp*. 2010;353(2–3):132–139.